# Properties of C1 and other ventrolateral medullary neurones with hypothalamic projections in the rat

Anthony J. M. Verberne*, Ruth L. Stornetta and Patrice G. Guyenet

*Department of Pharmacology, University of Virginia, Charlottesville, VA 22908, USA and* **University of Melbourne, Clinical Pharmacology and Therapeutics Unit, Austin & Repatriation Medical Centre, Heidelberg, 3084 Victoria, Australia*

(Received 13 October 1998; accepted after revision 17 February 1999)

1. This study compared (i) the properties of C1 cells with those of neighbouring non-C1 neurones that project to the hypothalamus and (ii) the properties of C1 cells that project to the hypothalamus with those of their medullospinal counterparts.

2. Extracellular recordings were made at three rostrocaudal levels of the ventrolateral medulla (VLM) in α-chloralose-anaesthetized, artificially ventilated, paralysed rats. Recorded cells were filled with biotinamide.

3. Level I (0–300 μm behind facial nucleus) contained spontaneously active neurones that were silenced by baro- and cardiopulmonary receptor activation and virtually unaffected by nociceptive stimulation (firing rate altered by $< 20\%$). These projected either to the cord (type I; 36/39), or to the hypothalamus (type II; 2/39) but rarely to both (1/39).

4. Level II (600–800 μm behind facial nucleus) contained (i) type I neurones ($n = 3$) (ii) type II neurones ($n = 11$), (iii) neurones that projected to the hypothalamus and were silenced by baro- and cardiopulmonary receptor activation but activated by strong nociceptive stimulation (type III, $n = 2$), (iv) non-barosensitive cells activated by weak nociceptive stimulation which projected only to the hypothalamus (type IV, $n = 9$), (v) cells that projected to the hypothalamus and responded to none of the applied stimuli (type V, $n = 7$) and (vi) neurones activated by elevating blood pressure which projected neither to the cord nor to the hypothalamus (type VI, $n = 4$).

5. Level III (1400–1600 μm behind facial motor nucleus) contained all the cell types found at level II except type I.

6. Most of type I and II (17/26) and half of type III cells (4/8) were C1 neurones. Type IV–V were rarely adrenergic (2/12) and type VI were never adrenergic (0/3).

7. All VLM baroinhibited cells project either to the cord or the hypothalamus and virtually all (21/23) C1 cells receive inhibitory inputs from arterial and cardiopulmonary receptors.

The C1 group of adrenergic neurones is located within the ventrolateral medulla (VLM) just below the ventral respiratory group (VRG). The C1 cell column extends from the caudal end of the facial motor nucleus to approximately the level of the obex (Hokfelt *et al.* 1984). Caudal to the obex, an increasing proportion of VLM catecholaminergic neurones do not express phenylethanolamine *N*-methyl transferase (PNMT) and are considered to be noradrenergic (A1 cells). The most rostrally located C1 neurones project to the thoracic spinal cord where they selectively target the intermediolateral cell column and lamina X (Ross *et al.* 1984; Milner *et al.* 1988; Minson *et al.* 1990). Their discharge properties *in vivo* have been well characterized (e.g. Brown & Guyenet, 1985; Lipski *et al.* 1995, 1996*a*; Schreihofer & Guyenet, 1997). Briefly, these neurones are tonically active, are powerfully inhibited by elevation of arterial blood pressure and have a pulse-modulated discharge at elevated levels of arterial blood pressure. These cells respond to a variety of visceral, somatic and supramedullary inputs in a manner that closely mimics the effects of these inputs on the peripheral sympathetic vasomotor outflow (for reviews see Guyenet *et al.* 1996; Sun, 1996). For these reasons, the bulbospinal C1 cells are assumed to contribute an excitatory drive to the preganglionic neurones that control sympathetic tone to the heart and blood vessels.

The C1 cells that project to the hypothalamus and basal forebrain (Sawchenko & Swanson, 1982; Tucker *et al.* 1987; Petrov *et al.* 1993; Otake *et al.* 1995) are largely distinct from the bulbospinal ones (Haselton & Guyenet, 1990). These cells are probably more numerous than their bulbospinal

counterparts (Minson *et al.* 1990) and are concentrated in the caudal part of the C1 group (Tucker *et al.* 1987). In contrast to the bulbospinal C1 cells, the input–output properties of the C1 cells that project to the hypothalamus and basal forebrain are largely unknown, especially from a neurophysiological standpoint. Judging from the results of c-fos expression studies in several species, the discharges of some of these neurones may be increased by moderate systemic hypotension (Li & Dampney, 1994), by both hypotension and hypertension (Chan & Sawchenko, 1998), by haemorrhage and by hypoxia (McAllen *et al.* 1992; Erickson & Millhorn, 1994). Collectively, brainstem catecholaminergic afferents to the paraventricular nucleus (PVN) and supraoptic nucleus (SON) (A1, A2, and C1 cells) are thought to contribute to the regulation of corticotrophin-releasing hormone, vasopressin and adrenocorticotrophic hormone via actions on the hypothalamo-pituitary system (Cunningham *et al.* 1990; Herman & Cullinan, 1997). The specific information carried by each catecholaminergic group is poorly known because of a lack of cellular neurophysiological data. VLM neurones with projections to the hypothalamus have been recorded in a few studies (Kaba *et al.* 1986; Kannan *et al.* 1986; McAllen & Blessing, 1987; Yamashita *et al.* 1989; Li *et al.* 1992) but the phenotype of the recorded cells could not be ascertained and therefore the specific properties of the adrenergic neurones could not be conclusively determined.

The present study was designed to identify the discharge characteristics of the C1 cells that project to the hypothalamus using a method that allows determination of the phenotype of a large proportion of the recorded cells (Schreihofer & Guyenet, 1997). One goal was to compare the properties of these C1 cells with those of neighbouring non-catecholaminergic neurones that also project to or through the hypothalamus. The second goal was to compare the properties of C1 cells that project to the hypothalamus with those of their spinally projecting counterparts. Our approach was to characterize the physiological properties of single VLM neurones antidromically activated from the thoracic cord or the caudal hypothalamus and to label them with biotinamide using the juxtacellular technique (Pinault, 1996; Schreihofer & Guyenet, 1997). Subsequently, C1 cells were identified by the presence of PNMT. Noradrenergic cells (A1) were identified by the presence of tyrosine hydroxylase (TH) and the absence of PNMT.

## METHODS

### General procedures

Experiments were performed on 28 male Sprague–Dawley rats (260–342 g) in accordance with NIH and Institutional Animal Care and Use Guidelines. Animals were anaesthetized initially by placement into a vessel containing halothane vapour (5%). The trachea was cannulated and all animals were ventilated artificially with 100% $O_2$ (1 ml (100 g body weight)$^{-1}$, 40–60 breaths min$^{-1}$) containing 1·3–1·5% halothane. This concentration of halothane produced a deep surgical level of anaesthesia and was maintained throughout the entire surgical procedure. The depth of anaesthesia was verified by noting the absence of responses to firm paw pinch and corneal probing. Core temperature was maintained at 36–38 °C. Arterial blood pressure was measured from the left carotid artery and drugs were injected via the left jugular vein. An inflatable snare was placed around the subdiaphragmatic abdominal aorta and was used to increase arterial blood pressure in order to stimulate arterial baroreceptors (Brown & Guyenet, 1985). Concentric bipolar stimulation electrodes were placed bilaterally on the mandibular branch of the facial nerves to elicit an antidromic field potential in the facial motor nucleus (Brown & Guyenet, 1985). To determine the axonal projections of the recorded cells, a bipolar stimulating electrode (SNEX-100, Rhodes Medical Instruments Inc., Woodland Hills, CA, USA) was inserted into the caudal hypothalamus (co-ordinates from bregma: −2·5 mm AP, 1·0 mm lateral to the mid-line, −9·0 mm below surface of dura mater) and a second one into the dorsolateral quadrant of the cord (T3 level). Stimulation parameters were 0·5–1 Hz, 0·5 ms duration and 0·3–2·5 mA intensity.

After all surgery was completed, the halothane was discontinued and α-chloralose (70 mg kg$^{-1}$, I.V.) was administered slowly. After ensuring that this dose of α-chloralose produced an appropriate level of anaesthesia, the paralysing agent pancuronium bromide (1 mg kg$^{-1}$, I.V., with 0·3–0·5 mg kg$^{-1}$ supplements as required) was administered. After the induction of neuromuscular blockade, the adequacy of the anaesthesia was judged by the stability of the arterial blood pressure and the absence of a pressor response to firm toe pinch. Additional α-chloralose (20–25 mg kg$^{-1}$, I.V.) was administered every 60 min or more frequently if required. Some recordings were made while the animals were ventilated with 100% oxygen and others while the animals were ventilated with room air. The resting blood pressure was 125 to 135 mmHg under pure oxygen and 100–115 mmHg under room air.

### Extracellular single-unit recordings

Extracellular single-unit recordings were made with glass electrodes filled with a 1·5% (w/v) solution of biotinamide (Molecular Probes) in 0·5 M NaCl as previously described (Schreihofer & Guyenet, 1997). These electrodes had an impedance in brain of 20–40 MΩ. The collision test was used to test whether constant latency spikes evoked by stimulation were antidromic (Lipski, 1981; Haselton & Guyenet, 1989). Neurones were labelled using the juxtacellular labelling technique (Pinault, 1996; Schreihofer & Guyenet, 1997). An Axoprobe 2A intracellular amplifier (Axon Instruments) was used in bridge mode (bandpass DC to 10 kHz) to record the extracellular discharges of VLM neurones. The signal was amplified and filtered (400–4000 Hz) and monitored on an oscilloscope. To label neurones, positive current pulses were delivered through the electrode for 1–6 min (200 ms duration, 5 Hz). Current intensity (0·3–4·0 nA) was adjusted to the minimum necessary to produce the rhythmic entrainment of the unit (Schreihofer & Guyenet, 1997).

Recordings were made in the ventrolateral medulla bilaterally at three rostrocaudal levels based on movements of the micropositioner carrying the recording microelectrode: (i) 0–300 μm caudal to the facial motor nucleus (level I; 11·8 mm caudal to bregma; Paxinos & Watson, 1986), (ii) 700–900 μm caudal to level I (level II; 12·5 mm caudal to bregma), and (iii) 700–900 μm caudal to level II (level III; 13·1 mm caudal to bregma). Level I was identified in relation to the caudal end of the facial motor nucleus which was mapped by recording antidromic field potentials (Brown & Guyenet, 1985). At most, one neurone per level on each side of the medulla was labelled with biotinamide so that labelled neurones could be unambiguously identified upon histological examination. Recordings were made using a dorsal transcerebellar approach. A

range of tests was applied to each cell in order to identify their projection patterns and physiological properties. These included: (i) elevation of arterial blood pressure by gradual subdiaphragmatic aortic occlusion (ii) stimulation of cardiopulmonary receptors using phenylbiguanide (PBG; 10 $\mu$g kg$^{-1}$, I.V.), (iii) activation of peripheral nociceptors by brief pinch applied to the hindquarters or tail, (iv) hypothalamic stimulation to test for antidromic activation, and (v) spinal stimulation to test for antidromic activation of a spinal projection. Brief pinch consisted of paw compression applied for less than 2 s with a needle holder. Light pinch consisted of paw compression that was non-painful if applied to a skin fold on one's person. This stimulus never elicited a change in blood pressure. Strong paw pinch implied a very firm compression of the paw of the type used to gauge the level of anaesthesia. Such a stimulus elicited a change in blood pressure of 5–15 mmHg. All spontaneously active neurones were tested for barosensitivity and hypothalamic or spinal projection. Silent cells projecting to the hypothalamus were detected by the presence of an antidromic spike elicited by hypothalamic stimulation.

### Immunocytochemistry

After completion of the experiment, the rats were deeply anaesthetized with urethane and perfused through the aorta with 250 ml phosphate-buffered normal saline (pH 7·4) followed by 500 ml 10% formaldehyde in 0·1 M phosphate buffer (pH 7·4) solution. The brains were removed and post-fixed for up to 72 h at 4 °C in the fixative solution. Coronal sections (40 $\mu$m) were cut through the medulla oblongata on a vibratome.

Biotinamide-filled neurones were identified by incubating the sections with streptavidin conjugated to alkaline phosphatase (Vector Laboratories, Burlingame, CA, USA; 1 : 1000 in 0·1 M Tris-saline, pH 7·4–0·1% Triton X-100). After rinsing the sections in Tris-saline (3×; 0·1 M, pH 7·4), they were pre-incubated in NMT (0·1 M Tris-HCl, pH 9·5, 0·1 M NaCl, 50 mM $MgCl_2$) and then reacted (6–15 min) with 4-Nitroblue Tetrazolium and 5-bromo-4-chloro-3-indolyl phosphate 4-toluidine salt (450 and 175 $\mu$g ml$^{-1}$, respectively; Boehringer Mannheim) in NMT containing levamisole (1 drop per 5 ml reaction mixture; Vector Laboratories) to inhibit endogenous alkaline phosphatase. The reaction was stopped by rinsing the sections in Tris-EDTA (3×; 0·1 M Tris, pH 8·5, 1 mM EDTA). The sections were then rinsed in Tris-saline (3×; 0·1 M, pH 7·4), mounted onto uncoated glass slides, dried, and coverslips were applied with Vectashield (Vector Laboratories). The sections that contained labelled neurones and their processes were identified under the light microscope and only those were processed for the detection of PNMT immunoreactivity (PNMT-ir). This procedure minimized the cost of the PNMT antibody.

To detect PNMT-ir, the sections were rinsed in Tris-saline (3×; 0·1 M, pH 7·4) and incubated first in Tris-saline (0·1 M, pH 7·4) containing 10% normal goat serum and Triton X-100 (0·1%). They were then incubated with a PNMT antibody for 3 h at room temperature or overnight at 4 °C (1 : 1000 in Tris-saline–10% normal goat serum–0·1% Triton X-100; rabbit polyclonal, Incstar Corporation, Stillwater, MN, USA). The sections were then rinsed in Tris-saline (3×; 0·1 M, pH 7·4) and incubated for 45 min with an indocarbocyanine dye-tagged secondary antibody (1 : 500 in Tris-saline–10% normal goat serum–0·1% Triton X-100; Cy-3-conjugated AffiniPure F(ab′)2 fragment goat anti-rabbit IgG; Jackson ImmunoResearch Labs Inc., West Grove, PA, USA). After rinsing in Tris-saline (3×; 0·1 M, pH 7·4), the sections were mounted onto uncoated slides, dried, and coverslips applied with Vectashield. The sections were examined with a fluorescence microscope.

Sections which contained neurones or processes which were biotinamide positive but were PNMT negative were processed further for TH immunoreactivity (TH-ir). TH-ir was identified by incubation of the sections in 10% normal goat serum–0·1% Triton X-100–0·1 M Tris-saline, pH 7·4, followed by incubation with an anti-TH antibody (1 : 1000 in Tris-saline–10% normal goat serum–0·1% Triton X-100; mouse monoclonal, Chemicon, Temecula, CA, USA) for 3 h at room temperature. After rinsing the sections in Tris-saline (3×; 0·1 M, pH 7·4), they were incubated with a secondary antibody (1 : 200 in Tris-saline–10% normal goat serum–0·1% Triton X-100; goat anti-mouse IgG tagged with Alexa 488; Molecular Probes) for 45 min. The sections were then rinsed in Tris-saline (3×; 0·1 M, pH 7·4), mounted onto uncoated slides, dried and coverslips were applied with Vectashield. Finally, the sections were examined under a fluorescence microscope.

The caudal hypothalamus of all the rats was sectioned coronally and the location of the tip of the recording electrode was examined after staining a one in four series of sections with Cresyl Violet.

The outline of histological sections, major nuclei and the location of the neurones of interest were mapped under a fluorescence microscope using a Ludl motor driven stage in combination with the Neurolucida software (Microbrightfield, Colchester, VT, USA) as described previously (Schreihofer & Guyenet, 1997). Neuroanatomical nomenclature is after Paxinos & Watson (1986).

### Data analysis and statistics

Arterial blood pressure, single-unit discharge and stimulation pulses were recorded on a video cassette recorder in PCM format (Vetter Instruments, Rebersburg, PA, USA). A microcomputer-based data acquisition system (AxoScope, Axon Instruments) was used to convert stored data into the formats used for display. Peri-stimulus time histograms and analyses of pulse synchrony were constructed using custom designed software (Guyenet *et al.* 1987). Axonal conduction velocities were calculated by dividing antidromic latencies by the straight-line distance between stimulation and recording electrodes (35 mm for thoracic cord, 11 mm for hypothalamus). All results are expressed as means ± standard error of the mean. Conduction velocity and firing rate data were compared by one-way ANOVA followed by Scheffé's test. $P < 0·05$ was considered as the level of significance.

### Drugs

$\alpha$-Chloralose (Fisher Scientific, Fair Lawn, NJ, USA) was dissolved (30 mg ml$^{-1}$) in 2% sodium tetraborate. Phenylephrine, phenylbiguanide and sodium nitroprusside were dissolved in normal saline (0·9% w/v NaCl) and administered intravenously in doses of 5–15, 10 and 10–20 $\mu$g kg$^{-1}$, respectively.

## RESULTS

### Distribution of PNMT-immunoreactive neurones in the ventrolateral medulla

Coronal sections from two brains were processed for the simultaneous detection of PNMT-ir and TH-ir in order to identify the proportion of C1 and A1 neurones present at the three medullary levels where units were recorded. Alternate sections were Nissl stained to obtain detailed anatomical information. Figure 1 shows representative coronal sections through each of the three levels (immunohistochemistry at left, Nissl stain at right). Level I (Fig. 1*Aa* and *Ab*) was characterized by a prominent nucleus ambiguus (compact portion, am) and a small or barely visible inferior

olive (IO). At this level, all TH-ir neurones in the VLM were PNMT positive. Level II (Fig. 1*Ba* and *Bb*) was characterized by a well-developed inferior olivary nucleus, a barely detectable nucleus ambiguus and the presence of the nucleus linearis (li). At this level of the VLM, again all TH-ir neurones were PNMT-ir. The third level (level III; Fig. 1*Ca* and *Cb*) was characterized by the presence of the forking rostral tips of the lateral reticular nucleus (LRN) ventrally and by the area postrema (AP) dorsally. At this level, the overwhelming majority of the TH-ir neurones were still PNMT positive. Cells counts were made to determine precisely the ratio between C1 (PNMT and TH positive) and A1 cells (TH positive but PNMT negative) at this level. In six sections from three rats, we counted 307 C1 cells (bilateral counts) and only 19 A1 neurones. Figure 2 illustrates the appearance of a C1 neurone (Fig. 2*A* and *B*) and of an A1 neurone (Fig. 2*C* and *D*). A1 neurones became predominant in the VLM only 500 $\mu$m caudal to the most caudal level at which recordings were made (level not illustrated). In summary, only C1 neurones are found in the VLM at levels I and II. At level III, C1 neurones still make up 95% of the total population of VLM catecholaminergic neurones.

### Neuronal search strategy

All neurones were recorded from 1·6 to 2·1 mm lateral to the mid-line using a dorsal approach. Neurones of the ventral respiratory group (VRG) with characteristic on–off

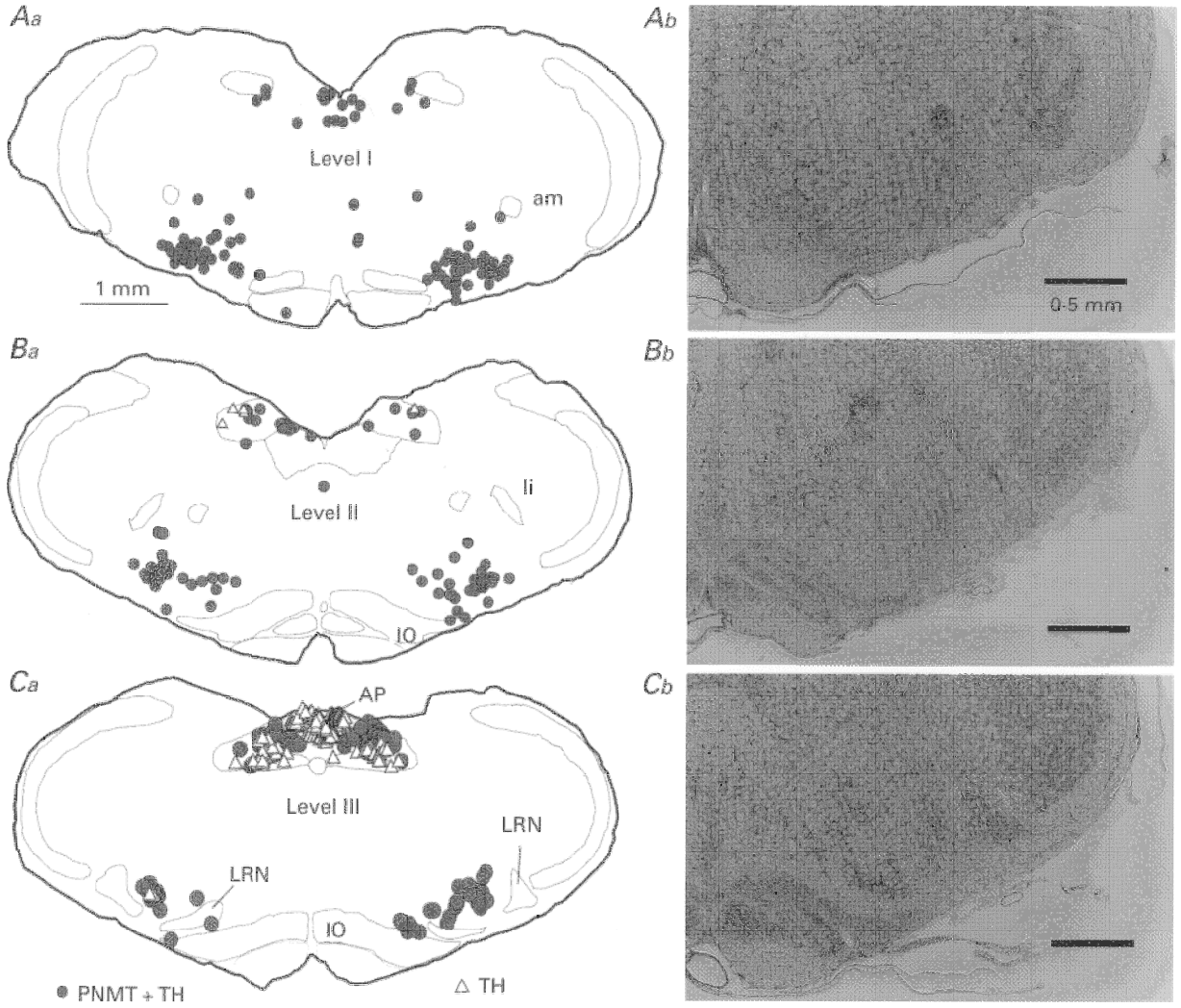


**Figure 1. Distribution of neurones immunoreactive for both PNMT and TH (C1 cells) and neurones containing only TH immunoreactivity (A1 cells)**

Distribution is shown at the three rostrocaudal levels where the electrophysiological recordings were made. Level I is just caudal to the facial motor nucleus (*Aa*; 11·8 mm caudal to bregma, co-ordinate after Paxinos & Watson, 1986), level II at an intermediate rostrocaudal location (*Ba*; 12·5 mm caudal to bregma), and level III at the level of the rostral border of the lateral reticular nucleus (*Ca*; 13·1 mm caudal to bregma). Corresponding Nissl-stained sections are shown for comparison (*Ab–Cb*). Abbreviations: am, nucleus ambiguus, compact portion; AP, area postrema; IO, inferior olive; li, nucleus linearis; LRN, lateral reticular nucleus.

respiratory discharges were encountered first. These cells were ignored but their presence was used as a landmark because most of the cells of interest were recorded at the lower edge of the VRG and within 500 $\mu$m below. The study focused exclusively on (i) VLM neurones that were either silenced or strongly activated by elevations of arterial blood pressure and (ii) any cell that projected to the cord or the hypothalamus, regardless of their barosensitivity. Other types of cells were frequently encountered in the VLM and were ignored. Continual stimulation of the hypothalamus was used to detect silent neurones with axonal projections to, or through, the hypothalamus. One hundred and three neurones were studied. We attempted labelling with biotinamide in 58 neurones. Forty-nine (85%) biotinamide-labelled neurones were successfully recovered following histology.

The 103 recorded neurones were classified into six well-demarcated categories: (i) cells silenced by blood pressure elevation which projected to the cord (type I), (ii) cells silenced by blood pressure elevation, with weak somatic input, and which projected to the hypothalamus (type II), (iii) cells silenced by blood pressure elevation, activated by nociceptive stimulation, and projecting to the hypothalamus (type III), (iv) non-barosensitive cells with prominent somatic input which projected to the hypothalamus (type IV), (v) cells unresponsive to any of the applied stimuli which projected to the hypothalamus (type V) and (vi) neurones activated by elevated arterial blood pressure, which projected neither to the hypothalamus nor the cord (type VI). All six neuronal types were usually not recorded in each animal. However, four and sometimes five neuronal types were encountered during a single experiment.

### Bulbospinal cells silenced by elevating arterial pressure (type I)

All active VLM neurones that were silenced by elevation of arterial blood pressure had projections either to the thoracic cord or to the hypothalamus ($n = 71$).

Type I cells (bulbospinal and barosensitive, Fig. 3) were generally active at rest although occasionally (2/43) they were silent and became active only when arterial blood pressure was lowered below the resting level with sodium nitroprusside. When spontaneously active, they were silenced by elevating arterial blood pressure from resting to 130–150 mmHg (Fig. 3*Aa*), they were silenced by administration of PBG (29/29 cells tested; Fig. 3*Ab*) and they were orthodromically activated by hypothalamic stimulation (Fig. 3*Ae* and *Bb*, top panels). All were activated antidromically by spinal cord stimulation (Fig. 3*Ac*). Antidromic and orthodromic spikes had virtually the same configuration (Fig. 3*Ad*). Orthodromic activation from the hypothalamus was completely occluded when arterial blood pressure was elevated (Fig. 3*Ae* and *Bb*, bottom panels). Under these conditions, hypothalamic stimulation did not elicit constant latency antidromic spikes suggesting that the cell did not project to the hypothalamus (Fig. 3*Bb*). In

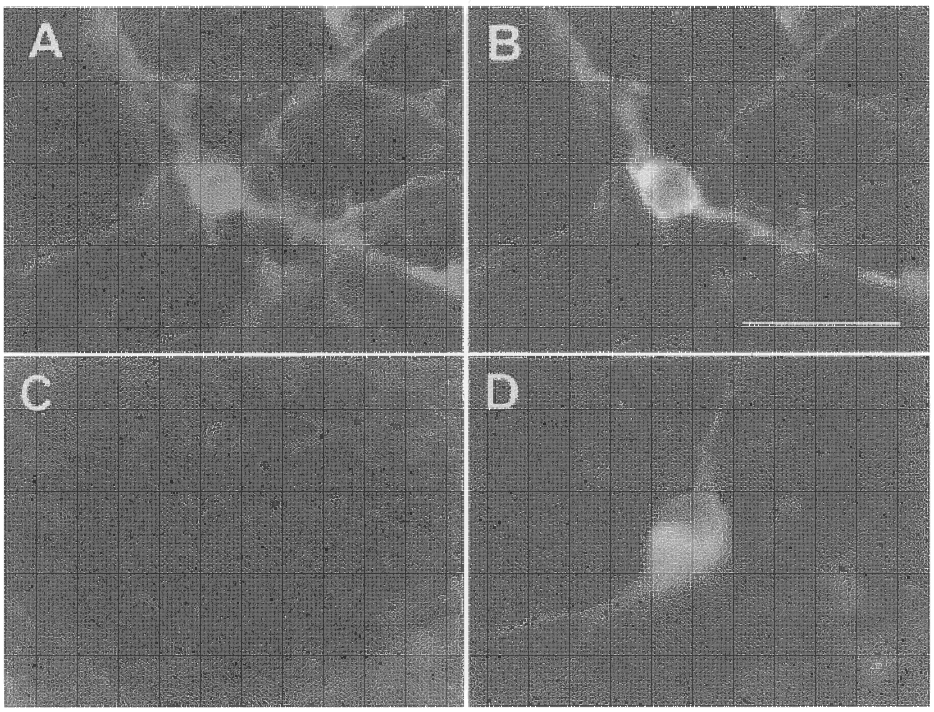


**Figure 2. Immunohistochemical identification of C1 and A1 neurones of the ventrolateral medulla**

PNMT-ir (A) and TH-ir (B) in a C1 neurone. Absence of PNMT-ir (C) and presence of TH-ir (D) in an A1 neurone. Scale bar, 25 $\mu$m.

contrast, antidromic spikes elicited by spinal cord stimulation were not blocked by arterial blood pressure elevation (Fig. 3*Bb*). The same absence of hypothalamic projection was found in 38 of 39 bulbospinal barosensitive neurones recorded.

Type I cells responded to nociceptive stimulation (strong pinch of hind foot, hind leg or tail) by a modest and short-lasting inhibition (not greater than 1 s duration; 0–20% reduction from resting discharge rate) or excitation (not greater than 1 s duration; 0–20% increase over resting discharge rate; not illustrated). These stimuli produced little or no increase in blood pressure (5–15 mmHg).

Type I cells were found commonly at level I, more rarely at level II (3/17) and never at level III (Fig. 4*A*). The mean

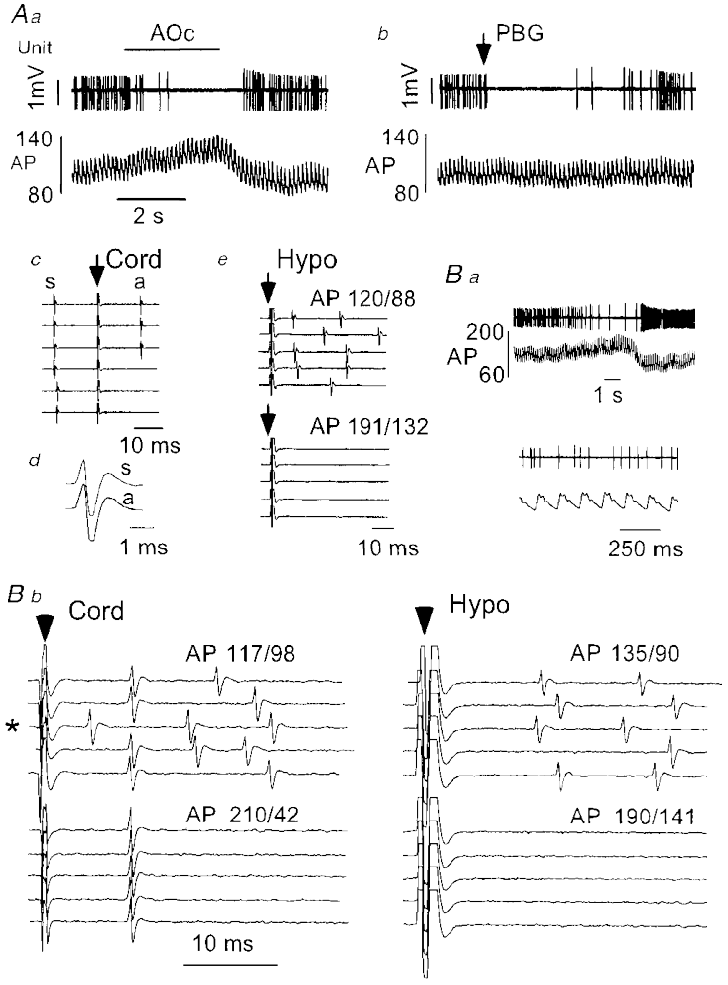


**Figure 3. Physiological properties of a type I phenotypically identified C1 neurone**

*Aa*, elevation of arterial blood pressure (AP, mmHg) by gradual aortic occlusion (AOc) resulted in inhibition of the discharge of this cell. *Ab*, cardiopulmonary receptor stimulation (PBG, 10 $\mu$g kg$^{-1}$, I.V.) briefly silenced the discharge of this neurone. *Ac*, constant latency antidromic spike (a) elicited by spinal cord stimulation (arrow; traces 1–3 from top). The delay between the spontaneous spike (s) and the spinal stimulus exceeds the critical interval for collision. Reduction of the delay between the spontaneous spike and the spinal stimulus to the critical interval results in collision of the antidromic spike (traces 4–6). *Ad*, configurations of the spontaneous (s) and antidromic spikes (a). *Ae*, hypothalamic stimulation (arrow) at resting arterial blood pressure (AP: 120/88 mmHg) results in orthodromic activation of the cell that is abolished by AP elevation (aortic occlusion). Note the absence of constant latency spikes. *Ba*, a second example of a type I barosensitive cell. The discharge of the cell was reduced during arterial blood pressure elevation (aortic occlusion). The discharge of the cell at resting arterial blood pressure is also shown on an expanded time scale. *Bb*, spinal cord stimulation (left panel) at resting arterial blood pressure elicits constant latency (antidromic) spikes (traces 1, 2, 4 and 5) as well as orthodromic responses. Collision of the antidromic spike with a spontaneous spike is evident in trace 3 (marked with an asterisk). Elevation of arterial blood pressure eliminates orthodromic driving but not antidromic activation. Hypothalamic stimulation (right panel) elicits only orthodromic spikes which are eliminated by arterial blood pressure elevation. No constant latency spikes are evident.

**Table 1. Conduction velocities and basal discharge rates of type I–V neurones**

| Neuronal type* | Group | No. | Conduction velocity † ($m\ s^{-1}$) | Firing rate (Hz) |
|---|---|---|---|---|
| I | Total‡ | 43 | 3·1 ± 0·3 (0·47–8·8) | 11 ± 1 (0–30) |
| | $PNMT^+$ | 9 | 2·7 ± 0·9 (0·56–8·8) | 9·9 ± 2·6 (1–23) |
| | $PNMT^-$ | 5 | 4·0 ± 0·6 (2·2–5·4) | 4 ± 3 (0–15) |
| II | Total | 15 | 0·42 ± 0·02 (0·29–0·65)§ | 2·0 ± 0·4 (0–5)§ |
| | $PNMT^+$ | 8 | 0·38 ± 0·02 (0·29–0·48) | 1·3 ± 0·4 (0–3) |
| | $PNMT^-$ | 4 | 0·49 ± 0·06 (0·39–0·65) | 1·4 ± 0·7 (0–3) |
| III | Total | 11 | 0·35 ± 0·03 (0·22–0·52)§ | 5 ± 1 (0–19) |
| | $PNMT^+$ | 4 | 0·31 ± 0·03 (0·26–0·39) | 4·3 ± 1·7 (1–9) |
| | $PNMT^-$ | 4 | 0·31 ± 0·05 (0·22–0·39) | 5 ± 3 (0–14) |
| IV | Total | 17 | 1·2 ± 0·2 (0·26–2·8)§ | 2 ± 1 (0–8)§ |
| | $PNMT^+$ | 1 | 0·42 | 1 |
| | $PNMT^-$ | 6 | 1·35 ± 0·42 (0·33–2·6) | 1·5 ± 1·0 (0–6) |
| V | Total | 8 | 0·39 ± 0·04 (0·23–0·65)§ | 1·1 ± 0·4 (0–2)§ |
| | $PNMT^+$ | 1 | 0·35 | 0·25 |
| | $PNMT^-$ | 4 | 0·43 ± 0·08 (0·23–0·65) | 0·6 ± 0·4 (0–1·5) |

* Type I, cells silenced by blood pressure elevation and which projected to the cord; type II, cells silenced by blood pressure elevation, virtually unaffected by nociceptive somatic stimulation, and projecting to the hypothalamus; type III, cells silenced by blood pressure elevation, vigorously activated by nociceptive stimulation and projecting to the hypothalamus; type IV, non-barosensitive cells vigorously activated by somatic stimuli and projecting to the hypothalamus; type V, cells unresponsive to any of the applied stimuli which project to the hypothalamus. † Conduction velocities of spinal axon of type I neurones and of hypothalamic axon of type II–V neurones. Values are means ± S.E.M. with ranges shown in parentheses. ‡ Totals for each cell type include phenotypically and non-phenotypically identified neurones. § $P < 0·05$ compared with corresponding values for type I cells (one-way ANOVA followed by Scheffé's test).

axonal conduction velocity and mean discharge rate of these neurones are shown in Table 1. The conduction velocities of type I neurones were significantly greater than those of type II–V neurones ($P < 0·05$; Table 1). Similarly, the discharge rates of type I neurones were significantly greater than those of types II, IV and V neurones ($P < 0·05$). The conduction velocities of type I neurones varied from 0·47 to 8·8 $m\ s^{-1}$ denoting a mixture of unmyelinated and lightly myelinated axons.

### Hypothalamus-projecting cells silenced by arterial pressure elevation (types II and III)

Neurones with projections to the hypothalamus and silenced by elevating mean arterial blood pressure in the 125–140 mmHg range were rarely found at level I (2/39) but they were commonly found at levels II and III (Fig. 4*A* and *B*). We include in this category a few neurones ($n = 5$) that were silent at resting arterial blood pressure and became active when blood pressure was lowered with

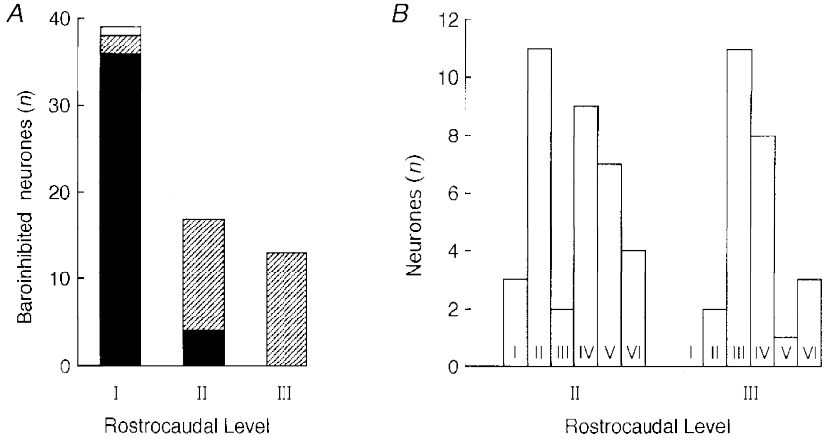


**Figure 4. Location of all recorded neurones**

*A*, rostrocaudal distribution of cells silenced by elevation of arterial blood pressure with projections to the spinal cord or the hypothalamus (i.e. types I, II and III only). Filled section, spinally projecting cells; hatched section, hypothalamus-projecting cells; open section, cells projecting to both spinal cord and hypothalamus. *B*, comparison of the distribution of cell types I–V I at levels II and III.

sodium nitroprusside. Neurones with projections to the hypothalamus and which were silenced by elevating mean arterial blood pressure were subclassified into two groups depending on whether they were unaffected (type II) or vigorously activated (type III) by nociceptive stimulation.

Figure 5 depicts the properties of a type II cell phenotypically identified as a C1 neurone. The cell shown in Fig. 5*A–D* illustrates the case of a neurone that was recorded in a rat ventilated with room air and which exhibited a typically lower resting arterial blood pressure (Fig. 5*B*; 100–105 mmHg). This cell was discharging at 4 Hz and was silenced by elevating arterial blood pressure. It was inhibited by cardiopulmonary receptor activation (Fig. 5*A*, PBG, 10 $\mu$g kg$^{-1}$) but was not noticeably affected by nociceptive stimulation. Figure 5*B* illustrates the relationship between arterial blood pressure and spike discharge rate. The cell was antidromically activated by hypothalamic stimulation (Fig. 5*C*) but spinal cord stimulation produced only orthodromic excitation (Fig. 5*D*). Figure 5*D* shows the effect of stimulation of the spinal cord and the occlusion of orthodromic spikes by elevation of systemic pressure by aortic occlusion. Note that stimulation of the cord did not evoke constant latency spikes when pressure was elevated. This criterion was used to conclude that the cell did not project to the thoracic spinal cord.

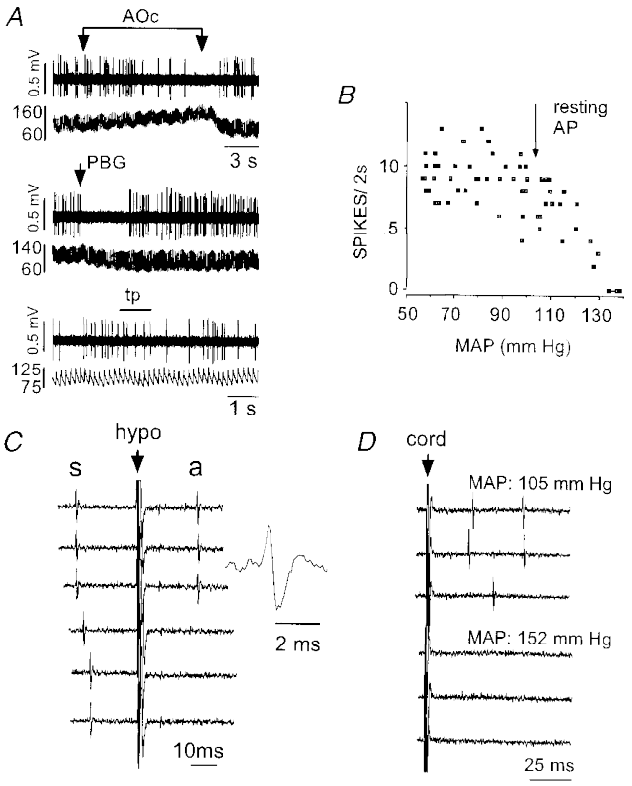


**Figure 5. Physiological properties of a type II phenotypically identified C1 neurone recorded in a rat ventilated with room air**

*A*, inhibition by aortic occlusion (AOc) (top two traces), I.V. injection of phenylbiguanide (PBG, 10 $\mu$g kg$^{-1}$, middle pair of traces) and insensitivity to nociceptive stimulation (toe pinch, tp; bottom pair of traces). In each pair of traces, the top trace shows the unit activity and the bottom trace AP (mmHg). *B*, relationship between discharge rate and mean arterial blood pressure. *C*, antidromic activation by hypothalamic stimulation. Hypothalamic stimulation (at arrow) triggered by the occurrence of a spontaneous spike (s) elicits constant latency antidromic spikes (a; top three traces). Stimulation within the critical latency results in collision of the antidromic spike (bottom three traces). The inset shows an enlargement of the antidromic spike. *D*, orthodromic driving (top three traces) produced by stimulation of the spinal cord (at arrow) was abolished by elevation of arterial blood pressure (bottom three traces). Peak to peak amplitude of spikes in *C* and *D*: 0·8 mV.

Figure 6 depicts the properties of another type II C1 cell recorded in an animal ventilated with 100% oxygen

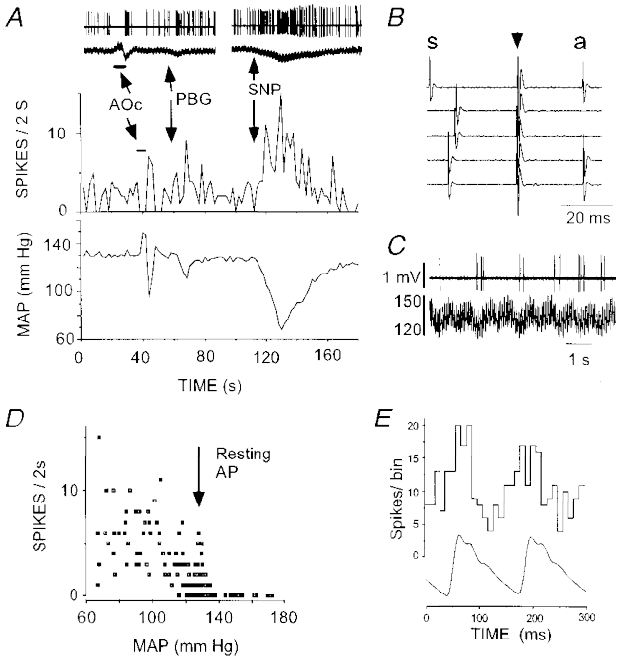


**Figure 6. Physiological properties of a type II phenotypically identified C1 neurone recorded in a rat ventilated with 100% oxygen**

*A*, inhibition by aortic occlusion (AOc) (top two traces show raw data) and I.V. injection of phenylbiguanide (PBG, 10 $\mu$g kg$^{-1}$). Reduction of arterial blood pressure (sodium nitroprusside, SNP) produced powerful activation of the cell. *B*, antidromic activation produced by hypothalamic stimulation. Hypothalamic stimulation (arrow) triggered by the spontaneous spike (s) elicits constant latency (antidromic, a) spikes (traces 1, 4 and 5). Stimulation within the critical interval after occurrence of the spontaneous spike results in collision (traces 2 and 3). *C*, apparent 'respiratory rhythm' of the discharge rate. Top trace, unit activity; bottom trace, AP (mmHg). *D*, relationship between discharge rate and mean arterial blood pressure (note higher resting AP compared with cell recorded under room air in Fig. 5). *E*, pulse-triggered histogram of unit discharge. In *A–C*, peak to peak amplitude of spikes is 1·4 mV.

(resting AP: 128 mmHg). This cell was inhibited by elevation of arterial blood pressure and cardiopulmonary receptor activation (Fig. 6*A*) and could be antidromically activated by hypothalamic stimulation (Fig. 6*B*). The relationship between discharge rate and mean arterial blood pressure was very similar to that of C1 cells recorded at lower resting blood pressure (compare Fig. 5*B* and Fig. 6*D*). However, under 100% oxygen, the cells were discharging at a slower and more irregular rate (1–2 Hz) and they were powerfully activated by lowering arterial blood pressure with sodium nitroprusside (Fig. 6*A*). This cell also displayed a respiratory or pump rhythm in its discharge rate (Fig. 6*C*). The discharge of type II cells was clearly pulse synchronous (Fig. 6*E*) when examined at resting blood pressures above 115 mmHg ($n = 5$). Little or no pulse synchrony was observed in 7 type II cells examined at resting arterial blood pressure of less than 110 mmHg.

Group data for type II neurones are shown in Table 1. The mean axonal conduction velocity of their hypothalamic projection was $0{\cdot}42 \pm 0{\cdot}02$ m s$^{-1}$ (Table 1) indicating that these neurones have unmyelinated axons. The majority of type II cells (10/14) were inhibited by cardiopulmonary receptor stimulation. The remaining cells were activated (3/14) or unaffected (1/14) by this stimulus. Stimulation of the hypothalamus and/or the spinal cord elicited orthodromic activation in most type II cells. Orthodromic spikes evoked from both locations could be abolished by elevation of arterial blood pressure.

Type III neurones projected to the hypothalamus (Fig. 7*B*) but not to the spinal cord. Figure 7 illustrates the case of a neurone that was not PNMT-ir. Type III neurones presented characteristics similar to those of type II (barosensitivity, inhibition by cardiopulmonary receptor stimulation; Fig. 7*A*) but their defining characteristic was a vigorous excitation during the application of a nociceptive stimulus to the tail or foot. This excitation was occluded at elevated arterial blood pressure (Fig. 7*C*), the occlusion usually being complete upon raising mean arterial blood pressure to approximately 160 mmHg. The sensitivity of type III cells to nociceptive stimulation could not be accounted for by a lighter level of anaesthesia as the nociceptive stimulus produced the usual lack of or minimal change in resting blood pressure (Fig. 7*C*). Most type III cells (10/13) were inhibited by cardiopulmonary receptor stimulation, while a few were modestly activated (3/13; $<20\%$). Group data on type III neurones are found in Table 1. Their mean axonal conduction velocity was $0{\cdot}35 \pm 0{\cdot}03$ m s$^{-1}$ indicating that the rostrally projecting axons of these neurones were unmyelinated.

### Hypothalamus-projecting, non-barosensitive cells with somatic input (type IV)

Type IV cells were activated antidromically by hypothalamic stimulation and responded to paw pinch with a brisk increase in discharge. In contrast to type III cells, type IV cells responded vigorously to even a light pinch of the foot and had a clear-cut receptive field usually consisting

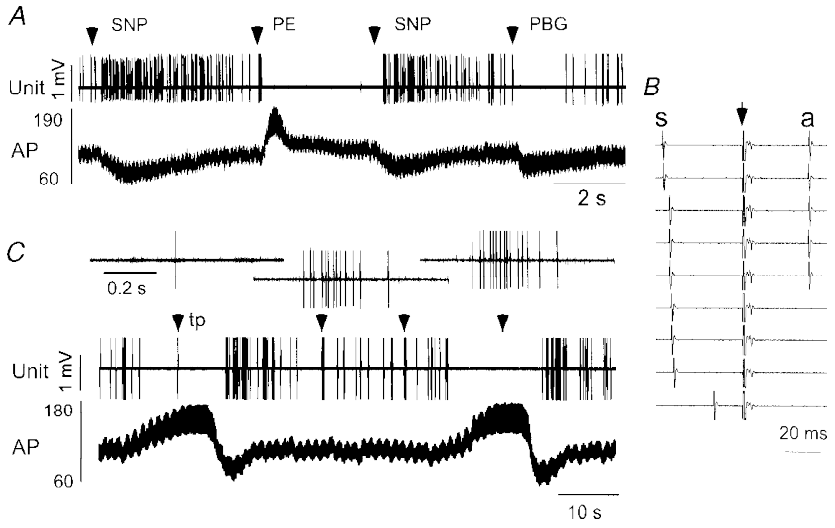


**Figure 7. Physiological properties of a type III non-C1 neurone**

*A*, lowering arterial blood pressure (AP, mmHg) with the vasodilator agent sodium nitroprusside (SNP) increased the discharge rate of this neurone. The opposite effect was produced by increasing AP with phenylephrine (PE). Administration of phenylbiguanide (PBG, 10 $\mu$g kg$^{-1}$, I.V.) inhibited the cell. *B*, antidromic activation produced by hypothalamic stimulation. Hypothalamic stimulation (arrow) triggered by the spontaneous spike (s) elicits constant latency (antidromic, a) spikes (traces 1–5). Stimulation within the critical interval after occurrence of the spontaneous spike results in collision (traces 6–9). *C*, toe pinch elicits a burst of action potentials that was markedly and reversibly reduced by simultaneous elevation of AP (aortic occlusion). The three insets at the top of *C* represent the response of the cell to the three first toe pinches at an expanded scale.

of the contralateral hindquarter and the root of the tail (Fig. 8*Aa*). These cells were unaffected by innocuous stimulation (brushing of the hair, passive movement of the hindleg). Type IV cells were typically silent (10/17) or very slowly active (< 3 Hz) at resting blood pressure (3/17) and none was activated by lowering blood pressure. When spontaneously active, these cells were insensitive to changes in AP or to cardiopulmonary receptor stimulation with PBG. Figure 8 shows that even extreme elevation of AP did not reduce the excitation produced by toe pinch in type IV cells. This characteristic permitted the discrimination of type IV neurones from type III cells, even if the latter were silent. Type IV cells were vigorously activated orthodromically from the thoracic cord (Fig. 8*C*). No evidence of antidromic activation could be observed but spinal projection could not be ruled out because antidromic spikes could have been occluded by the numerous orthodromic action potentials elicited by even low intensity stimulation of the cord. Type IV neurones had a mean axonal conduction velocity of 1·2 ± 0·2 m $s^{-1}$ (range = 0·26–2·8 m $s^{-1}$; $n = 17$) suggesting that some of these neurones could have lightly myelinated axons (Table 1).

### Unresponsive cells with hypothalamic projection (type V)

Type V neurones did not respond to arterial blood pressure manipulations (Fig. 9*Aa* and *Ba*), cardiopulmonary receptor stimulation (Fig. 9*Bb*) or nociceptive stimuli (Fig. 9*Ba*), or responded with small and inconsistent changes in discharge rate. These cells were either silent or discharged infrequently (1·1 ± 0·4 Hz, $n = 8$) and this made the tests of responsivity difficult. However, 6/7 cells tested were unaffected by PBG while 1 was inhibited slightly. Figure 9*A* shows a typical example later identified as non-catecholaminergic. A very frequent characteristic of type V cells illustrated in Fig. 9*Ab* and *Ac* was a prominent dissociation of the initial segment spike (IS) from the somatodendritic (SD) spike (IS–SD break) upon hypothalamic stimulation with frequent complete failure of the SD component. The mean axonal conduction velocity of the hypothalamic projection of these cells was 0·39 ± 0·04 m $s^{-1}$ (range = 0·23–0·65 m $s^{-1}$; $n = 8$) and indicates that their axons are unmyelinated (Table 1).

### Neurones activated by elevated arterial blood pressure (type VI)

Neurones activated by elevated arterial blood pressure (type VI) were found at levels II (4/7) and III (3/7) but not at level I (Fig. 4). Type VI neurones were barely active at resting pressure. Their discharge rate increased linearly with the mean arterial blood pressure above a threshold of 100–110 mmHg (Fig. 10*Bb*). This threshold was the same as that at which type I–III cells were inhibited. Type VI cells were strongly pulse modulated (Fig. 10*Bc*) and they were also silenced by lowering blood pressure with sodium

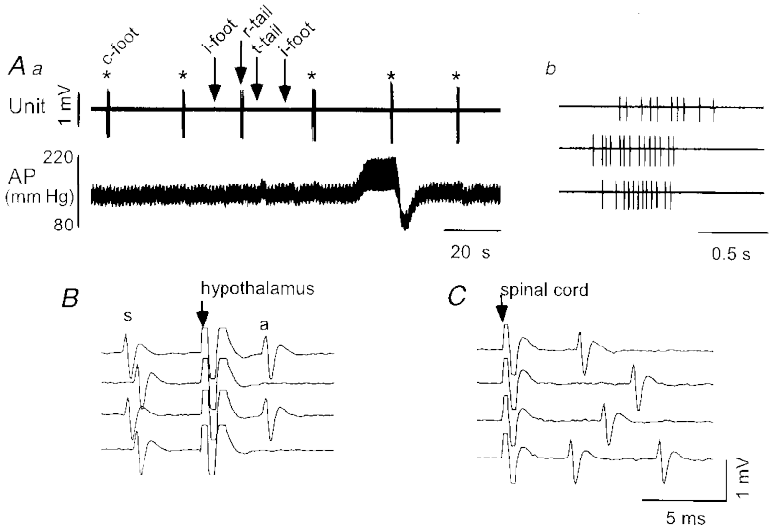


**Figure 8. Physiological properties of a type IV neurone**

*Aa*, nociceptive stimulation of the contralateral hind paw (*, c-foot) elicits a burst of action potentials and little alteration of resting arterial blood pressure (AP). Noxious stimulation applied to the ipsilateral hind paw (i-foot) and tip of the tail (t-tail) has no effect while pinch of the root of the tail (r-tail) also elicits a burst of spikes. AP elevation (aortic occlusion) does not inhibit the toe pinch-evoked burst. *Ab*, expanded time scale view of the burst of spikes elicited by the second, fourth and fifth applications of noxious contralateral paw pinch. *B*, collision of the antidromic spike (a) elicited by hypothalamic stimulation (arrow) with the spontaneous spike (s). In the first and third traces, the delay between the spontaneous spike and the hypothalamic stimulus exceeds the critical interval for collision. Reduction of the delay between the spontaneous spike and the hypothalamic stimulus to the critical interval results in collision of the antidromic spike. *C*, spinal cord stimulation results in only orthodromic stimulation of the cell.

nitroprusside (Fig. 10*Aa* and *Ab*). The linear relationship between mean blood pressure and discharge rate, the invariant firing threshold from one trial to the next (Fig. 10*Ba*), and the lack of spike amplitude change during blood pressure elevation (Fig. 10*Ab*) were used as evidence that the effect of blood pressure on these cells was due to synaptic activity and not to mechanical artifacts. Stimulation of cardiopulmonary afferents with PBG generally produced either excitation (5/7; Fig. 10*Aa* and *Ab*) or no effect (Fig. 10*Ba*). In the case illustrated in Fig. 10*Ba*, the inhibition occurred after PBG administration and was probably due to the drop in arterial blood pressure and consequent baroreceptor unloading.

Type VI neurones could not be antidromically activated from either the thoracic cord or the hypothalamus.

### Phenotype of recorded neurones

Juxtacellular application of biotinamide to a physiologically characterized unit labelled a single neurone. Labelling of more than one cell was extremely rare and these cases were excluded from the study because of ambiguity in the identification of the cell.

Figure 11 illustrates the histological appearance of a biotinamide-labelled type I cell under tungsten light (Fig. 11A1 and A2, biotinamide) and fluorescence illumination (Fig. 11A3, neurone is devoid of PNMT-ir). The dark material immediately below this neuron was an artifact associated with a small amount of damage caused by the microelectrode. Fig. 11B1–3 shows an example of a biotinamide-labelled type II neurone which was immunoreactive for PNMT. Figure 12 illustrates the location, phenotype and projection pattern of all recovered cells.

As indicated in Table 1, 64% (9/14) of type I, two-thirds of type II (8/12) and half of type III neurones (4/8) were found to contain PNMT-ir. Collectively, 62% (21/34) of the cells that were silenced by arterial blood pressure elevation (types I–III) were C1 cells. Type I–III cells devoid of PNMT-ir were found at all levels and were intermingled with the C1 neurones. None of these cells contained TH-ir.

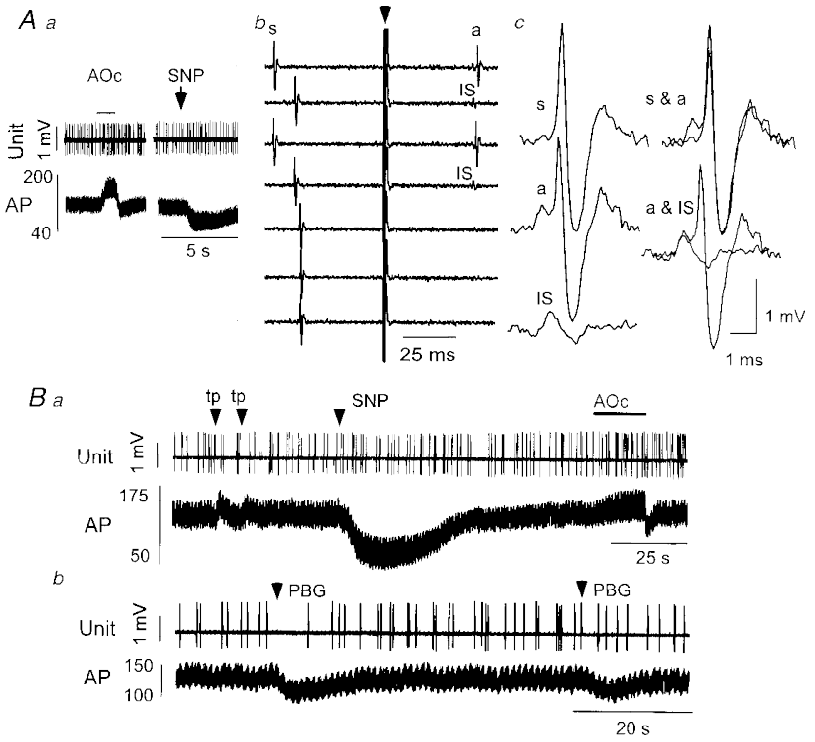


**Figure 9. Physiological properties of a type V neurone**

*Aa*, elevation or reduction of arterial blood pressure (AP, mmHg) using aortic occlusion (AOc) or sodium nitroprusside (SNP) does not alter the discharge rate of this neurone. *Ab*, hypothalamic stimulation (arrow) applied outside the critical period after occurrence of a spontaneous spike (s) elicits an antidromic spike (a, top four traces) which frequently fails to invade the soma (IS in the second and fourth traces from top). Hypothalamic stimulation applied within the critical period after the spontaneous spike fails to elicit an antidromic spike (bottom three traces). *Ac*, left column, spontaneous spike (s), antidromic spike (a) and initial segment of antidromic spike (IS). *Ac*, right column, superposition of spontaneous and antidromic spike (top) and superposition of antidromic spike and antidromic initial segment (bottom). *Ba*, toe pinch elicits small increases in arterial blood pressure but fails to alter unit discharge consistently. *Bb*, cardiopulmonary receptor stimulation with phenylbiguanide (PBG, 10 $\mu$g kg$^{-1}$, I.V.) has no consistent effect on discharge rate.

In contrast, the occurrence of PNMT-ir in the remaining types was much less frequent: 1/7 type IV, 1/5 type V and 0/3 type VI.

### Location of hypothalamic stimulation sites

All stimulation electrode tracks were found within the hypothalamus at the level of the ventromedial hypothalamic nucleus. A representative location is depicted in Fig. 13.

## DISCUSSION

Several investigators have reported the presence of neurones inhibited by arterial blood pressure elevation among a mixed population of VLM neurones with projections to the hypothalamus (Kannan *et al.* 1986; McAllen & Blessing, 1987; Li *et al.* 1992). The present study provides an anatomical description of these various classes of cells and identifies the specific physiological properties of the adrenergic neurones.

### Methodological considerations

The TH and PNMT antibodies used in the present study both produced a very strong and specific stain of cell bodies, dendrites and terminals. Immunohistochemistry for TH and PNMT used fluorophores with non-overlapping spectral characteristics and each marker could be detected without interference from the other.

To maximize the chance of recovering biotinamide-labelled neurones, we used a chromogenic option based on the use of alkaline phosphatase which, in preliminary experiments, was found to be more sensitive than the use of a streptavidin-conjugated fluorophore. In cells that were lightly stained with biotinamide, there was no interference between the alkaline-phosphatase-derived chromogen and the detection of PNMT-ir (e.g. Fig. 11). In cells that were heavily stained with biotinamide, the opaque alkaline-phosphatase-derived chromogen did quench the fluorescence in the somata and proximal dendrites. However, the finer dendrites and axons of these heavily filled cells contained much lower levels of alkaline phosphatase-derived chromogen and the presence or absence of PNMT-ir in these processes could be reliably determined. Thus, we believe that the method used in this study produced very few false negatives.

The juxtacellular labelling method is based on the assumption that if only one cell is labelled at the site of recording, the labelled cell is the one that was recorded (Pinault, 1996). This assertion is consistent with our experience so far (Schreihofer & Guyenet, 1997). Firstly, we found that entrainment of a recorded cell is absolutely necessary to obtain filling. Secondly, in the rare instances when two cells are filled, a second unit becomes discriminated and entrained while the current pulses are delivered. Finally, in the RVLM, we find that the filled axons of bulbospinal neurones with slow conduction velocity ($< 1$ m s$^{-1}$) are always varicose while those of fast-conducting neurones are smooth, without varicosities and emerge from a typical initial segment (Schreihofer & Guyenet, 1997). Such a result could not be observed if labelling was not specific for the recorded neurone because bulbospinal cells with myelinated and unmyelinated axons are intermingled and found in equal proportion in the rostral VLM.

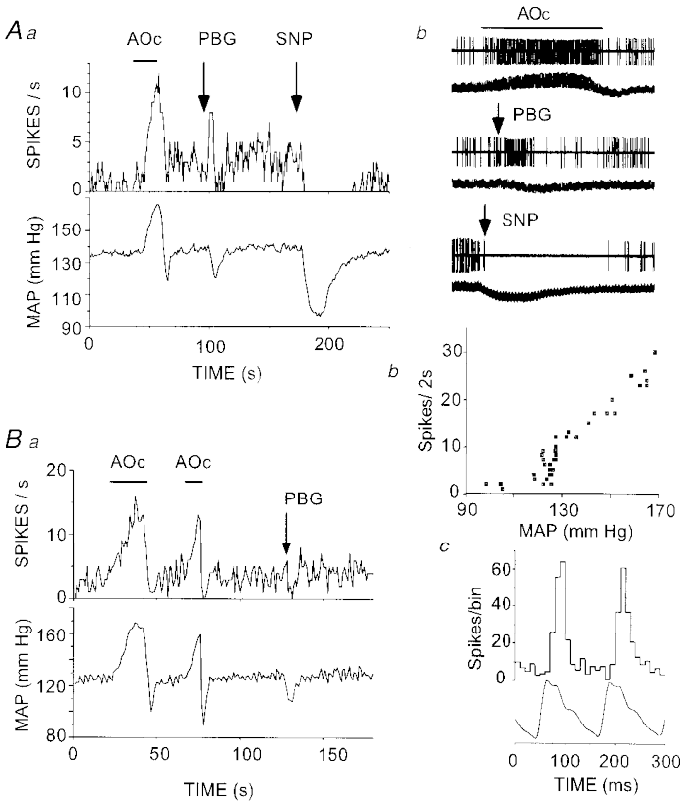


**Figure 10. Physiological properties of two type VI neurones**

*Aa* and *Ab*, increased neuronal discharge in response to elevation of mean arterial blood pressure (MAP) by aortic occlusion (AOc) and cardiopulmonary receptor stimulation with phenylbiguanide (PBG, 10 $\mu$g kg$^{-1}$, I.V.). Reduction of AP abolishes the neuronal discharge. In *Ab*, each pair of traces (unit activity at top, AP at bottom) represents an excerpt of the raw data used for panel *Aa*. The peak to peak amplitude of spikes is 1·2 mV, the top and middle pairs of traces each have a total duration of 28 s, and the bottom pair (SNP) has a total duration of 75 s. *Ba*, increased neuronal discharge in response to elevation of MAP. This cell did not react to PBG injection but it stopped firing after the injection when systemic blood pressure dropped. *Bb*, neuronal discharge is directly proportional to MAP beyond a threshold. *Bc*, pulse-synchronous discharge of type VI neurone.

Cells antidromically activated from the caudal hypothalamus in the present study may project to the hypothalamus as is the case for many C1 neurones (Sawchenko & Swanson, 1982; Tucker *et al.* 1987; Petrov *et al.* 1993; Otake *et al.* 1995) or to any of a number of structures located rostral to the stimulation point which receive brainstem projections through the medial forebrain bundle. Cells antidromically activated from either the spinal cord or hypothalamus were considered to be spinally projecting or hypothalamic-projecting cells, respectively. However, a limitation of the technique is that failure to detect antidromic activation is not proof of the absence of an axonal projection to the site of stimulation.

**Anatomical considerations**

The three levels of the VLM where recordings were made are functionally very heterogeneous. Level I corresponds to the rostral ventrolateral medulla region from which the largest pressor and sympathoexcitatory responses are evoked when glutamate is microinjected (Ruggiero *et al.* 1994). Dorsally, this region is characterized by the presence of Bötzinger neurones, and ventrally by the presence of a subset of C1 neurones projecting to the spinal cord (Ruggiero *et al.* 1994). Level II corresponds to the level of the pre-Bötzinger complex, a portion of the VRG thought to play a key role in respiratory rhythm generation in the neonate (Smith *et al.* 1991). Pressor responses from

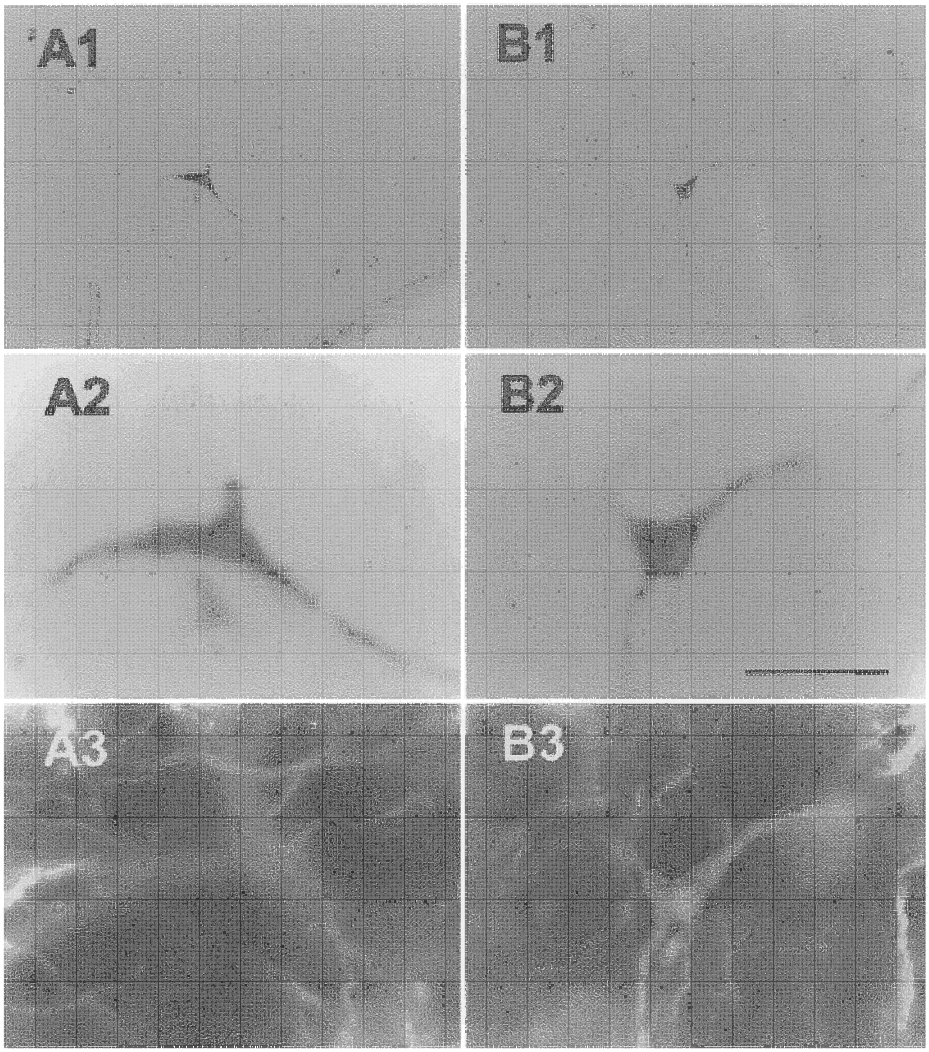


**Figure 11. Phenotypic characterization of VLM neurones**

A1, low power photomicrograph of a single biotinamide-labelled ventrolateral medullary barosensitive, medullospinal neurone (type I). A2, high power photomicrograph of cell in A1. The dark material immediately below this neuron was an artifact associated with a small amount of damage caused by the microelectrode. A3, same cell is devoid of PNMT immunofluorescence. B1, low power photomicrograph of a single biotinamide-labelled ventrolateral medullary barosensitive neurone projecting to the hypothalamus (type II). B2, high power photomicrograph of cell in B1. B3, same cell as in B1 and B2 displaying immunofluorescence for PNMT. Scale bar for A2, A3, B2 and B3 is 50 $\mu$m; scale bar for A1 and B1 is 200 $\mu$m.

injections of excitatory amino acids at this level of the VLM are much smaller than those elicited at level I (Ruggiero *et al.* 1994). Level III corresponds to the ventrolateral medullary depressor area, which is also referred to as the caudal ventrolateral medulla or CVL. Injections of glutamate at this level produce profound hypotension and microinjections of excitatory amino acid receptor antagonists into this site block the baroreflex (Guyenet *et al.* 1987).

Our immunohistochemical data indicate that the only catecholaminergic neurones present in the VLM at the two rostral levels investigated are C1 cells and that, even at the most caudal level investigated, the ratio between C1 and A1 neurones is still of the order of 20 to 1. These data are consistent with the fact that not one hypothalamus-projecting biotinamide-labelled neurone was found to be noradrenergic. The present data also suggest that the VLM level where the baroreflex can be blocked (Guyenet *et al.* 1987; Jeske *et al.* 1993) overlaps with the caudal end of the C1 group and only very little with the A1 neurones.

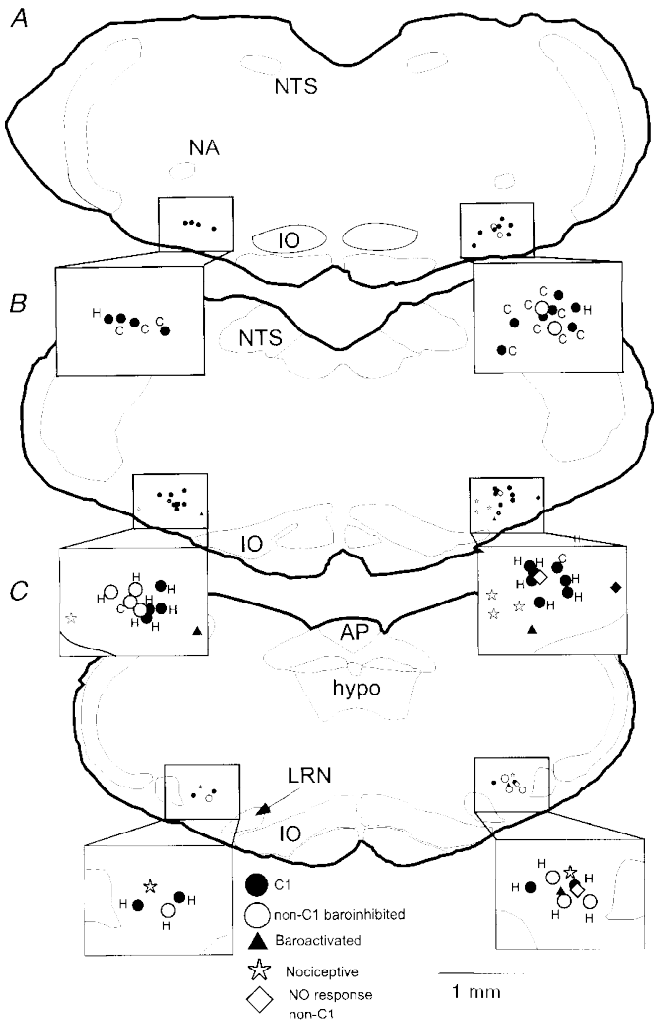


**Figure 12. Location, phenotype and projection pattern of histologically recovered neurones**

*A*, *B* and *C* depict neurones identified in levels I, II and III, respectively. ●, C1 cells (includes types I, II and III); ○, non-C1 barosensitive cells (types I, II and III); ▲, baroactivated cells (type VI); ☆, nociceptive cells (type IV); ◇, non-responsive, non-C1 cells (type V). Each inset shows an enlargement of the VLM area and identifies whether the baroinhibited cells have spinal (C) or hypothalamic (H) projections. Abbreviations: AP, area postrema; hypo, hypoglossal nucleus; IO, inferior olive; LRN, lateral reticular nucleus; NA, ambiguus nucleus; NTS, solitary tract nucleus.

### Properties common to all C1 neurones

Both populations of C1 neurones examined (bulbospinal, BS-C1, and projecting to the hypothalamus, HYP-C1) are generally active at rest and are powerfully inhibited by elevating arterial blood pressure by means of aortic coarctation. Under anaesthesia, brief aortic coarctation probably selectively activates arterial baroreceptors and ventricular mechanoreceptors. Both afferents trigger similar cardiovascular reflexes and have a high degree of convergence within the nucleus of the solitary tract (Paton, 1998).

Because the resting discharge of most C1 cells is typically less than the heart rate, pulse modulation of their firing can only be revealed by construction of pulse-triggered activity histograms. We also found that pulse modulation was present only when pressure was sufficiently above the baroreflex threshold to produce a significant degree of ongoing neuronal inhibition. This threshold was at least 100 mmHg under chloralose anaesthesia and, accordingly, pulse modulation at rest was observed only when recordings were made in the presence of 100% $O_2$, which resulted in a resting level of arterial blood pressure substantially above this threshold. The pulse modulation of the BS-C1 cells reflects pulse-related oscillations in the discharge of baroreceptor afferents (Brown & Guyenet, 1985). It is logical to extend this explanation to the HYP-C1 cells. The present evidence that the vast majority of C1 cells are inhibited by elevating arterial blood pressure is consistent with the interpretation of several c-fos studies performed in awake rats (Li & Dampney, 1994; Chan & Sawchenko, 1998). In the present study, we did not detect any C1 neurones that were activated by elevation of arterial blood pressure. The observation that up to 30% of C1 neurones express Fos following long-term (30 min) arterial blood pressure elevation with the vasoconstrictor agent phenylephrine suggests that this procedure may excite C1 cells via secondary reflexes or stress.

A second similarity between all C1 cells examined is the triphasic shape of their action potential and the fact that IS/SD dissociation was not observed in antidromic spikes. As a result, spontaneous and antidromic spikes had an almost identical configuration. This peculiarity separated C1 cells from another type of VLM neurone projecting to the hypothalamus (type V) that was generally unresponsive to our challenges and was generally not PNMT-ir.

A third similarity between all C1 cells is that orthodromic activation produced by stimulation of either the cord or the hypothalamus was completely occluded by baroreceptor

activation. This property clearly separated C1 cells from other VLM neurones with hypothalamic projections (e.g. type IV neurones). It is presumably due to the fact that baroreceptor activation produces a strong GABAergic postsynaptic inhibition in C1 cells which hyperpolarizes the neurones (Lipski *et al.* 1996*b*). GABAergic postsynaptic inhibition may shunt excitatory inputs which, in C1 cells, appear predominantly located in distal dendrites (Aicher *et al.* 1996). Occlusion of antidromic spikes by baroreceptor activation was never observed. In fact, observation of antidromic spikes in barosensitive cells was often facilitated by inhibition of the discharge of the cell produced by elevation of arterial blood pressure.

**Differences between C1 cells**

The first obvious difference between C1 adrenergic neurones with spinal or hypothalamic projection is the anatomical location. BS-C1 neurones were narrowly confined to the rostral tip of the VLM while HYP-C1 neurones were concentrated in the caudal two-thirds of the C1 cell group. This result is in general agreement with existing retrograde mapping data (Tucker *et al.* 1987).

The second difference is that all HYP-C1 neurones have unmyelinated axons (conduction velocity of less than 0·5 m $s^{-1}$) while, as shown by both electrophysiology and electron microscopy, the BS-C1 neurones have both unmyelinated and lightly myelinated axons (Morrison *et al.* 1988; Schreihofer & Guyenet, 1997). The present study confirms that all bulbospinal baroinhibited neurones of level I with axonal conduction velocity of less than 1 m $s^{-1}$ are C1 neurones while less than 50% of the baroinhibited neurones with faster conducting axons are C1 neurones (Schreihofer & Guyenet, 1997). Thus, only a subgroup of rostrally located C1 neurones that control sympathetic tone via their projection to the thoracic cord appear to have myelinated axons. We have previously shown that these neurones also have a generally higher rate of discharge than the unmyelinated BS-C1 neurones (Schreihofer & Guyenet, 1997). The functional significance of this phenotypic differentiation remains to be determined. In any case, the present study suggests that the C1 cells that project to the hypothalamus may be more closely related to the unmyelinated component of the bulbospinal adrenergic projection than to the other bulbospinal C1 cells.

Variability between C1 neurones was observed with respect to their response to stimulation of cardiopulmonary receptors with PBG. PBG is a 5-$HT_3$ receptor agonist (Veelken *et al.* 1990) that, when given into the jugular vein, probably stimulates a variety of vagal afferents including those arising from the right atrium, the right ventricle and the lungs (Hainsworth, 1991). Whereas all BS-C1 neurones were uniformly inhibited by PBG, a small proportion of the HYP-C1 cells (3/12) were activated. This suggests that there may be differences in the types of cardiopulmonary afferents these cells receive. Intra-carotid administration of 5-HT in anaesthetized cats produced excitation followed by inhibition of carotid body chemoreceptor discharge via a 5-$HT_3$ receptor-dependent mechanism (Kirby & McQueen, 1984). However, intravenous administration is likely to result in lower concentrations of PBG at carotid body 5-$HT_3$ receptors. Furthermore, when administered intravenously (jugular vein), PBG would first activate pulmonary and cardiac vagal afferents.

Variability between C1 neurones was also observed with respect to their response to noxious somatic stimulation. Rostral VLM barosensitive neurones are excited by somatic nociceptive inputs in other, probably more lightly anaesthetized preparations, in which nociceptive stimulation leads to an increase in blood pressure (Sun & Spyer, 1991). Our anaesthetic conditions were such that strong nociceptive stimulation produced little (5–15 mmHg) or no pressor effect which, in effect, means that the stimulus must have produced little or no sympathetic activation. The lack of reactivity of BS-C1 neurones to nociceptive stimulation is therefore in line with their presumed sympathoexcitatory function. In contrast, we found a population of HYP-C1 neurones confined largely to level III that were strongly activated by nociceptive stimulation. The present data suggest that the strength of the nociceptive somatic input to various groups of C1 neurones varies considerably.

**Non-catecholaminergic neurones inhibited by baroreceptor stimulation project to the hypothalamus**

Thirty-eight per cent of the recorded hypothalamus-projecting VLM neurones that were powerfully inhibited by activation of baroreceptors contained neither PNMT-ir nor TH-ir. One interpretation is that this percentage represents false negative results inherent to the juxtacellular labelling method. For reasons detailed above we do not think this interpretation is likely to be correct. In addition, our

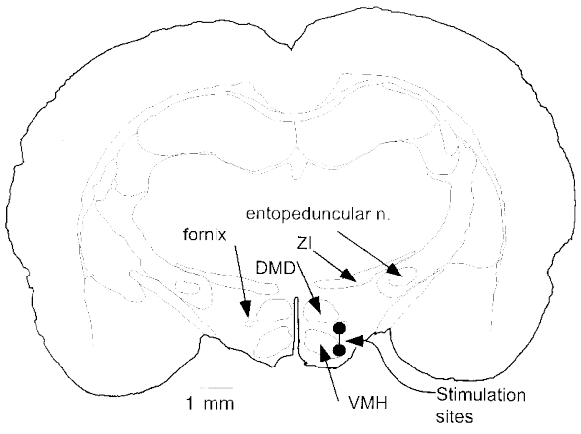


**Figure 13. Typical location of a hypothalamic stimulation site**

Large circles represent typical locations of inner and outer components of the concentric bipolar stimulation electrode. Abbreviations: DMD, diffuse area of the dorsomedial hypothalamic nucleus; VMH, ventromedial hypothalamic nucleus; ZI, zona incerta.

estimate of the proportion of C1 neurones among the fast-conducting bulbospinal and barosensitive neurones of the rostral VLM (about 50 %) is very similar to that obtained with an intracellular staining method (Lipski *et al.* 1995). Therefore, we are led to conclude that the VLM contains numerous non-catecholaminergic neurones that convey baroreceptor information to the hypothalamus and beyond. By analogy with the sympathetic vasomotor system, it is likely that the paraventricular and other barosensitive nuclei of the hypothalamus receive baroreceptor information via a mixture of C1 and non-catecholaminergic neurones.

### Neurones with nociceptive inputs and insensitivity to blood pressure (type IV )

VLM cells vigorously excited by nociceptive stimulation that project to or through the hypothalamus have been described in an earlier study (Kaba *et al.* 1986). These cells were found to be resistant to the neurotoxin 6-hydroxydopamine, which suggested that they were not noradrenergic (Kaba *et al.* 1986). We agree with this conclusion as we did not find any type IV neurone that was PNMT negative and TH positive. Furthermore, we also found that these cells were rarely of the C1 type (1/7). Further work is needed to determine where exactly these cells project and whether they might relay the excitatory effect of noxious stimulation (paw pinch and sciatic or femoral nerve stimulation) to SON vasopressin-secreting cells (Day & Sibbald, 1990).

### Baroactivated neurones of the VLM (type VI)

The baroactivated neurones recorded in the present study were not antidromically activated from the hypothalamus or the cord, and therefore these cells do not qualify as putative bulbospinal 'sympathoinhibitory' neurones. A more likely possibility is that these cells were either cardiovagal motor neurones (McAllen & Spyer, 1978) or the previously described propriomedullary interneurones which may be GABAergic and transmit baroreceptor afferent information to the bulbospinal sympathoexcitatory neurones of the rostral VLM (Guyenet, 1990; Terui *et al.* 1990; Jeske *et al.* 1993; Chan & Sawchenko, 1998). The baroactivated cells that we identified histologically were located well below the nucleus ambiguus suggesting that the second possibility (propriomedullary neurones) is more likely. The present results indicate that most of these cells receive convergent inputs from baroreceptors and cardiopulmonary receptors.

We did not find baroactivated neurones at level I where bulbospinal neurones with presumed sympathoexcitatory function are concentrated. This is consistent with the fact that very few if any cardiovagal motor neurones or baroactivated GABAergic neurones have been detected at this rostral level (Jeske *et al.* 1993; Standish *et al.* 1994; Chan & Sawchenko, 1998). In agreement with prior data (Chan & Sawchenko, 1998), we found baroactivated neurones in a more caudal location (levels II and III) where they are intermixed with baroinhibited neurones that project to the hypothalamus but rarely to the spinal cord. Though our results are in general agreement with the suggestion that the VLM contains cells that receive excitatory inputs from baroreceptors intermixed with cells that are inhibited by baroreceptor stimulation (Zagon & Spyer, 1996), we differ as to the interpretation. Specifically, we could not confirm the existence in the VLM of spinally projecting, baroactivated neurones which would qualify as putative sympathoinhibitory neurones (Deuchars *et al.* 1997). In addition, we found that baroactivated neurones have little or no overlap with the VLM bulbospinal neurones that are assumed to subserve a sympathoexcitatory function. Instead, we found that the baroactivated neurones were intermixed with the caudal half of the C1 group that contains neurones which project to the hypothalamus but rarely to the cord.

### Conclusion

In conclusion, the hypothalamic projection from VLM contains baroinhibited neurones that consist of a slight majority of C1 neurones interspersed with non-catecholaminergic neurones. The projection also includes several other types of non-catecholaminergic cells of unknown phenotype, one of which carries somatic nociceptive but not cardiopulmonary information. A very large majority of C1 neurones, irrespective of their projection, are strongly inhibited by baroreceptor stimulation and are generally also inhibited by cardiopulmonary afferents. Their response to nociceptive somatic input is highly variable and seems more pronounced within the caudal third of the C1 column. C1 cells that project to the hypothalamus most closely resemble the slow-conducting unmyelinated component of the BS spinal C1 cells with presumed sympathoexcitatory function.

Further experiments will be needed to determine whether the properties of A1 neurones that are located further caudally in the VLM and also project to the hypothalamus resemble those of the C1 cells.

Aicher, S. A., Saravay, R. H., Cravo, S., Jeske, I., Morrison, S. F., Reis, D. J. & Milner, T. A. (1996). Monosynaptic projections from the nucleus tractus solitarii to C1 adrenergic neurons in the rostral ventrolateral medulla: comparison with input from the caudal ventrolateral medulla. *Journal of Comparative Neurology* **373**, 62–75.

Brown, D. L. & Guyenet, P. G. (1985). Electrophysiological study of cardiovascular neurons in the rostral ventrolateral medulla in rats. *Circulation Research* **56**, 359–369.

Chan, R. K. W. & Sawchenko, P. E. (1998). Organization and transmitter specificity of medullary neurons activated by sustained hypertension: Implications for understanding baroreceptor reflex circuitry. *Journal of Neuroscience* **18**, 371–387.

Cunningham, E. T. Jr, Bohn, M. C. & Sawchenko, P. E. (1990). Organization of adrenergic inputs to the paraventricular and supraoptic nuclei of the hypothalamus in the rat. *Journal of Comparative Neurology* **292**, 651–667.

Day, T. A. & Sibbald, J. R. (1990). Noxious somatic stimuli excite neurosecretory vasopressin cells via A1 cell group. *American Journal of Physiology* **258**, R1516–1520.

Deuchars, S. A., Spyer, K. M. & Gilbey, M. P. (1997). Stimulation within the rostral ventrolateral medulla can evoke monosynaptic GABAergic IPSPs in sympathetic preganglionic neurons in vitro. *Journal of Neurophysiology* **77**, 229–235.

Erickson, J. T. & Millhorn, D. E. (1994). Hypoxia and electrical stimulation of the carotid sinus nerve induce fos-like immunoreactivity within catecholaminergic and serotoninergic neurons of the rat brainstem. *Journal of Comparative Neurology* **348**, 161–182.

Guyenet, P. G. (1990). Role of the ventral medulla oblongata in blood pressure regulation. In *Central Regulation of Autonomic Functions*, ed. Loewy, A. D. & Spyer, K. M., pp. 145–167. Oxford University Press, New York.

Guyenet, P. G., Filtz, T. M. & Donaldson, S. R. (1987). Role of excitatory amino acids in rat vagal and sympathetic baroreflexes. *Brain Research* **407**, 272–284.

Guyenet, P. G., Koshiya, N., Huangfu, D., Baraban, S. C., Stornetta, R. L. & Li, Y. W. (1996). Role of medulla oblongata in generation of sympathetic and vagal outflows. *Progress in Brain Research* **107**, 127–144.

Hainsworth, R. (1991). Reflexes from the heart. *Physiological Reviews* **71**, 617–658.

Haselton, J. R. & Guyenet, P. G. (1989). Electrophysiological characterization of putative C1 adrenergic neurons in the rat. *Neuroscience* **30**, 199–214.

Haselton, J. R. & Guyenet, P. G. (1990). Ascending collaterals of medullary barosensitive neurons and C1 cells in rats. *American Journal of Physiology* **258**, R1051–1063.

Herman, J. P. & Cullinan, W. E. (1997). Neurocircuitry of stress: Central control of the hypothalamo-pituitary-adrenocortical axis. *Trends in Neurosciences* **20**, 78–84.

Hokfelt, T., Johansson, O. & Goldstein, M. (1984). Central catecholamine neurons as revealed by immunohistochemistry with special reference to adrenaline neurons. In *Classical Transmitters in the CNS*, vol. 2, part I, ed. Bjorklund, A. & Hokfelt, T., pp. 157–276. Elsevier, Amsterdam.

Jeske, I., Morrison, S. F., Cravo, S. L. & Reis, D. J. (1993). Identification of baroreceptor reflex interneurons in the caudal ventrolateral medulla. *American Journal of Physiology* **264**, R169–178.

Kaba, H., Saito, H., Otsuka, K. & Seto, K. (1986). Ventrolateral medullary neurons projecting to the medial preoptic/anterior hypothalamic area through the medial forebrain bundle: an electrophysiological study in the rat. *Experimental Brain Research* **63**, 369–374.

Kannan, H., Osaka, T., Kasai, M., Okuya, S. & Yamashita, H. (1986). Electrophysiological properties of neurons in the caudal ventrolateral medulla projecting to the paraventricular nucleus of the hypothalamus in rats. *Brain Research* **376**, 342–350.

Kirby, G. C. & McQueen, D. S. (1984). Effects of the antagonists MDL 72222 and ketanserin on responses of cat carotid body chemoreceptors to 5-hydroxytryptamine. *British Journal of Pharmacology* **83**, 259–269.

Li, Y. W. & Dampney, R. A. L. (1994). Expression of fos-like protein in brain following sustained hypertension and hypotension in conscious rabbits. *Neuroscience* **61**, 613–634.

Li, Y. W., Gieroba, Z. J. & Blessing, W. W. (1992). Chemoreceptor and baroreceptor responses of A1 area neurons projecting to supraoptic nucleus. *American Journal of Physiology* **263**, R310–317.

Lipski, J. (1981). Antidromic activation of neurones as an analytical tool in the study of the central nervous system. *Journal of Neuroscience Methods* **4**, 1–32.

Lipski, J., Kanjhan, R., Kruszewska, B. & Rong, W. (1996*a*). Properties of presympathetic neurones in the rostral ventrolateral medulla in the rat: an intracellular study '*in vivo*'. *Journal of Physiology* **490**, 729–744.

Lipski, J., Kanjhan, R., Kruszewska, B., Rong, W. F. & Smith, M. (1996*b*). Pre-sympathetic neurones in the rostral ventrolateral medulla of the rat: electrophysiology, morphology and relationship to adjacent neuronal groups. *Acta Neurobiologiae Experimentalis* **56**, 373–384.

Lipski, J., Kanjhan, R., Kruszewska, B. & Smith, M. (1995). Barosensitive neurons in the rostral ventrolateral medulla of the rat *in vivo*: morphological properties and relationship to C1 adrenergic neurons. *Neuroscience* **69**, 601–618.

McAllen, R. M., Badoer, E., Shafton, A. D., Oldfield, B. J. & McKinley, M. J. (1992). Hemorrhage induces c-fos immunoreactivity in spinally projecting neurons of cat subretrofacial nucleus. *Brain Research* **575**, 329–332.

McAllen, R. M. & Blessing, W. W. (1987). Neurons (presumably A1-cells) projecting from the caudal ventrolateral medulla to the region of the supraoptic nucleus respond to baroreceptor inputs in the rabbit. *Neuroscience Letters* **73**, 247–252.

McAllen, R. M. & Spyer, K. M. (1978). The baroreceptor input to cardiac vagal motoneurones. *Journal of Physiology* **282**, 365–374.

Milner, T. A., Morrison, S. F., Abate, C. & Reis, D. J. (1988). Phenylethanolamine *N*-methyltransferase-containing terminals synapse directly on sympathetic preganglionic neurons in the rat. *Brain Research* **448**, 205–222.

Minson, J., Llewellyn-Smith, I., Neville, A., Somogyi, P. & Chalmers, J. (1990). Quantitative analysis of spinally projecting adrenaline-synthesising neurons of C1, C2 and C3 groups in rat medulla oblongata. *Journal of the Autonomic Nervous System* **30**, 209–220.

Morrison, S. F., Milner, T. A. & Reis, D. J. (1988). Reticulospinal vasomotor neurons of the rat rostral ventrolateral medulla: relationship to sympathetic nerve activity and the C1 adrenergic cell group. *Journal of Neuroscience* **8**, 1286–1301.

Otake, K., Ruggiero, D. A. & Nakamura, Y. (1995). Adrenergic innervation of forebrain neurons that project to the paraventricular thalamic nucleus in the rat. *Brain Research* **697**, 17–26.

Paton, J. F. R. (1998). Convergence properties of solitary tract neurones driven synaptically by cardiac vagal afferents in the mouse. *Journal of Physiology* **508**, 237–252.

Paxinos, G. & Watson, C. (1986). *The Rat Brain in Stereotaxic Coordinates*, 2nd edn. Academic Press, Sydney.

Petrov, T., Krukoff, T. L. & Jhamandas, J. H. (1993). Branching projections of catecholaminergic brainstem neurons to the paraventricular hypothalamic nucleus and the central nucleus of the amygdala in the rat. *Brain Research* **609**, 81–92.

Pinault, D. (1996). A novel single-cell staining procedure performed in vivo under electrophysiological control: morpho-functional features of juxtacellularly labeled thalamic cells and other central neurons with biocytin or neurobiotin. *Journal of Neuroscience Methods* **65**, 113–136.

Ross, C. A., Ruggiero, D. A., Joh, T. H., Park, D. H. & Reis, D. J. (1984). Rostral ventrolateral medulla: selective projections to the thoracic autonomic cell column from the region containing C1 adrenaline neurons. *Journal of Comparative Neurology* **228**, 168–185.

Ruggiero, D. A., Cravo, S. L., Golanov, E., Gomez, R., Anwar, M. & Reis, D. J. (1994). Adrenergic and non-adrenergic spinal projections of a cardiovascular-active pressor area of medulla oblongata: quantitative topographic analysis. *Brain Research* **663**, 107–120.

Sawchenko, P. E. & Swanson, L. W. (1982). The organization of noradrenergic pathways from the brainstem to the paraventricular and supraoptic nuclei in the rat. *Brain Research* **257**, 275–325.

Schreihofer, A. M. & Guyenet, P. G. (1997). Identification of C1 presympathetic neurons in rat rostral ventrolateral medulla by juxtacellular labeling in vivo. *Journal of Comparative Neurology* **387**, 524–536.

Smith, J. C., Ellenberger, H. H., Ballanyi, K., Richter, D. W. & Feldman, J. L. (1991). Pre-Botzinger complex: a brainstem region that may generate respiratory rhythm in mammals. *Science* **254**, 726–729.

Standish, A., Enquist, L. W. & Schwaber, J. S. (1994). Innervation of the heart and its central medullary origin defined by viral tracing. *Science* **263**, 232–235.

Sun, M. K. (1996). Pharmacology of reticulospinal vasomotor neurons in cardiovascular regulation. *Pharmacological Reviews* **48**, 465–494.

Sun, M. K. & Spyer, K. M. (1991). Nociceptive inputs into rostral ventrolateral medulla–spinal vasomotor neurones in rats. *Journal of Physiology* **436**, 685–700.

Terui, N., Masuda, N., Saeki, Y. & Kumada, M. (1990). Activity of barosensitive neurons in the caudal ventrolateral medulla that send axonal projections to the rostral ventrolateral medulla in rabbits. *Neuroscience Letters* **118**, 211–214.

Tucker, D. C., Saper, C. B., Ruggiero, D. A. & Reis, D. J. (1987). Organization of central adrenergic pathways: I. Relationships of ventrolateral medullary projections to the hypothalamus and spinal cord. *Journal of Comparative Neurology* **259**, 591–603.

Veelken, R., Sawin, L. L. & DiBona, G. F. (1990). Epicardial serotonin receptors in circulatory control in conscious Sprague–Dawley rats. *American Journal of Physiology* **258**, H466–472.

Yamashita, H., Kannan, H. & Ueta, Y. (1989). Involvement of caudal ventrolateral medulla neurons in mediating visceroreceptive information to the hypothalamic paraventricular nucleus. *Progress in Brain Research* **81**, 293–302.

Zagon, A. & Spyer, K. M. (1996). Stimulation of aortic nerve evokes three different response patterns in neurons of rostral VLM of the rat. *American Journal of Physiology* **271**, R1720–1728.

**Acknowledgements**

This work was supported by a grant from the National Institutes of Health to P.G.G. (HL 28785). A.J.M.V. is a Research Fellow of the National Health and Medical Research Council of Australia and was supported by a Clive & Vera Ramaciotti Foundations Travel Award while on study leave at the University of Virginia.

**Corresponding author**

P. G. Guyenet: Box 448 HSC, Department of Pharmacology, University of Virginia, Charlottesville, VA 22908, USA.

Email: pgg@virginia.edu